Fall 2009

Nona-arginine peptides facilitate cellular entry of semiconductor nanocrystals: mechanisms of uptake

Yi Xu

Department:

NONA-ARGININE PEPTIDES FACILITATE CELLULAR ENTRY OF SEMICONDUCTOR NANOCRYSTALS: MECHANISMS OF UPTAKE

by

YI XU

A THESIS

Presented to the Faculty of the Graduate School of the

MISSOURI UNIVERSITY OF SCIENCE AND TECHNOLOGY

In Partial Fulfillment of the Requirements for the Degree

MASTER OF SCIENCE IN APPLIED AND ENVIRONMENTAL BIOLOGY

2009

Approved by

Yue-Wern Huang, Advisor
Katie Shannon
Jeffrey Winiarz

ABSTRACT

Luminescent semiconductor quantum dots (QDs) have recently been used for delivering and monitoring biomolecules, such as drugs and proteins. However, QDs alone have a very low efficiency of transport across the plasma membrane. In order to increase the efficiency of QD delivery, synthetic nona-arginine (sR9) was used, a cell penetrating peptide, to facilitate uptake. Data demonstrated that sR9 could significantly increase the cellular uptake of QDs by noncovalent binding between QDs and sR9. Furthermore, the mechanisms of QD/sR9 cellular internalization were investigated. Low temperature and metabolic inhibitors markedly inhibited the uptake of QD/sR9, indicating that internalization is an energy-dependent process. Several pathway inhibitors and the RNAi technique were used to analyze the mechanism of uptake in live cell imaging studies. siRNA knockdown demonstrated that clathrin-, and caveolin-dependent endocytosis were not involved in QD/sR9 internalization. The conclusion is that the major routes of cellular uptake involve macropinocytosis and lipid-raft dependent process.

ACKNOWLEDGMENTS

I would like to thank my advisor Dr. Yue-wern Huang for his support, guidance and constant encouragement. Without his help, my thesis would never have been completed.

I would like to thank Dr. Katie Shannon and Dr. Jeffrey Winiarz for serving as my committee members, and for their input, guidance, help, and interest in this research.

I would like to thank Dr. Han-Jung Lee from National Dong Hwa University (Taiwan) for his collaboration, guidance, advice and comments on this research.

I greatly appreciated the assistance and support from my friends, Chuan-Chin Huang, Tien-Chun Wang, and Hsiu Jen Wang, all of whom gave me some helpful advice on my experiments. Thanks also to the faculty members, as well as other graduate students, in the Biological Department at Missouri University of Science & Technology for their support.

Finally, I would also like to thank my parents, Yuanjie Xu and Zengmei Miao, for their long-term encouragement and support of my graduate study. I want to thank my husband, Yi Zheng, for his support and constant encouragement. Without their love and support, I could not have completed my graduate study in the U.S.A.

TABLE OF CONTENTS

LIST OF ILLUSTRATIONS

LIST OF TABLES

1. INTRODUCTION

Fluorescent semiconductor quantum dots (QDs) have been used to deliver and monitor biomolecules into cells in the past few years (Hoshino *et al*., 2004; Bharali *et al*., 2005; Michalet *et al*., 2005). Advantages of QDs over traditional dyes and proteins (e.g., GFP, RFP) include, but are not limited to, their unique physical and chemical properties such as photostability, high quantum yield, narrow emission peak, exceptional resistance to degradation, and broad size-dependent photoluminescence (Alivisatos *et al*., 2005; Michalet *et al*., 2005). QDs properties such as multiplexing potential, photostability, and inorganic nature make them useful for delivering or monitoring biomolecules in live cells. However, although QDs could be engulfed into living cells, the intracellular concentration of QDs is not very high (Xue *et al*., 2007). Therefore, recently bio-conjugates or peptide-mediated QDs delivery were carried out to improve the internalization.

Cell penetrating peptides (CPPs), also known as protein transduction domains (PTDs) or membrane transduction peptides (MTPs), have been used for transduction of biologically active proteins, siRNA, and drugs across plasma membranes (Dietz and Bahr 2004; Wang *et al*., 2007). The advantages of CPPs include ease of preparation, lack of toxicity to the cell, and high efficiency of transduction (Tunnemann *et al*., 2008). CPPs can enter cells in a half-time of 1.8 minutes, corresponding to a first-order rate constant k of 0.007 sec-1 (Ziegler *et al*., 2005). Among many CPPs, the cellular uptake of polyarginine tends to be more efficient than that of polylysine, polyhistidine or polyornithine (Futaki, 2002). The highest translocation efficiency was reached by using octa-arginine or nona-arginine peptides (Futaki, 2002). sR9 has been shown to effectively

deliver not only covalently fused protein but also noncovalent mixed protein into different types of animal and plant cells (Wang *et al*., 2006; Wang *et al*., 2007).

The exact mechanism of cellular entry of CPPs is still under vigorous debate. Several reports previously showed that CPPs delivery of molecules into cells was independent of endocytosis, energy, receptors, or active transporters (Schwarze *et al*., 2000; Lindsay, 2002; Wadia and Dowdy, 2002). Later, it was found that fixing cells might have artificially transduced molecules across plasma membranes. More recent studies with live cell imaging suggested the mechanisms may involve macropinocytosis (Snyder and Dowdy, 2004; Chang *et al*., 2007).

The uptake mechanism of QDs is less-well studied. By using specific inhibitors, Ruan *et al*. identified macropinocytosis, actin filaments, and microtubules as required for of internalization and intracellular transport for streptavidin-coated QD/Tat-biotin in HeLa cells (Ruan *et al*., 2007). Zhang *et al*. demonstrated that carboxylic QDs were internalized by lipid rafts dependent endocytosis in human epidermal keratinocytes (HEKs), and these pathways were primarily regulated by the G-protein–coupled receptor associated pathway and low density lipoprotein receptor/scavenger receptor (Zhang and Monteiro-Riviere, 2009).

Our goals are to 1) test whether synthetic nona-arginine (sR9) can noncovalently facilitate QD uptake and 2) investigate the internalization mechanism of QD/sR9. We treated A549 cells with QDs alone and QD/sR9 complex, respectively, to demonstrate the efficiency uptake of QDs at the aid of sR9. Inhibitors and siRNA were used to study mechanism of uptake.

2. REVIEW OF LITATURE

2.1. INTRODUCTION OF QUANTUM DOTS

Quantum dots are colloidal nanocrystals with unique optical properties that make them outstanding fluorescent probes for long-term and multicolor imaging.

2.1.1. QD Anatomy. QDs consist of a semiconductor core, a passivation shell (usually made of ZnS), and additional coatings. The core is composed of periodic groups of II – VI (e.g. CdSe, CdTe, CdS, ZnSe), III – V (e.g. InP, InAs) or IV – VI (e.g. PbSe) (Figure 2.1). The size of the core is 2 to 10 nm. Figure 2.2 shows the size comparison of QDs and comparable objects. The size of QDs can increase dramatically depending on the coating layer around the core. A thin layer of ZnS on the nanoparticle surface protects the core from oxidation and increases the photoluminescence quantum yield (Michalet *et al*., 2005; Maysinger *et al*., 2007). The charge of the nanoparticles is determined by polar groups of the coating ligands and the surrounding pH.

QDs are mostly synthesized in nonpolar organic solvents, which make them insoluble in water. Their hydrophobic surface ligands must be replaced by hydrophilic ones for biological applications. QDs can also be prepared by water-based synthesis method, which creates hydrophilic surface ligands around the core.

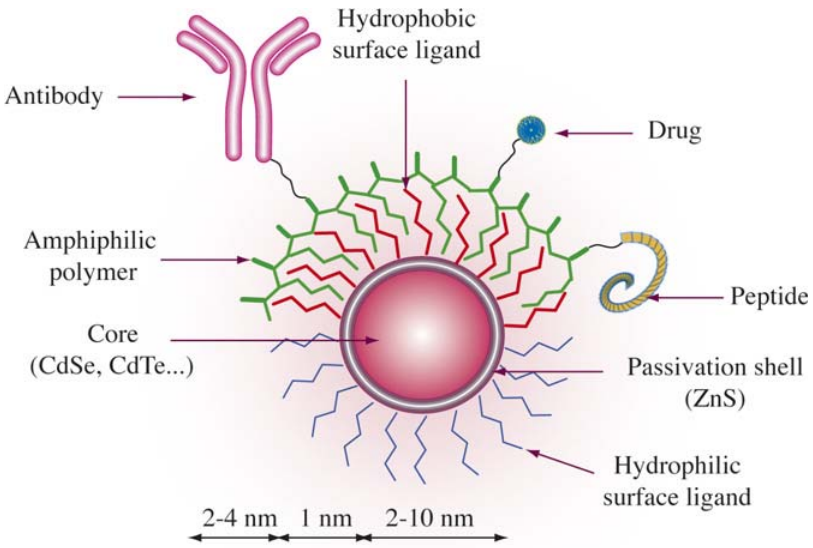

(Maysinger *et al*., 2007)

Figure 2.1. Anatomy of QDs. Surface modifications of QDs provide protection of the cores and QD targeting. Such modifications considerably enhance QD sizes.

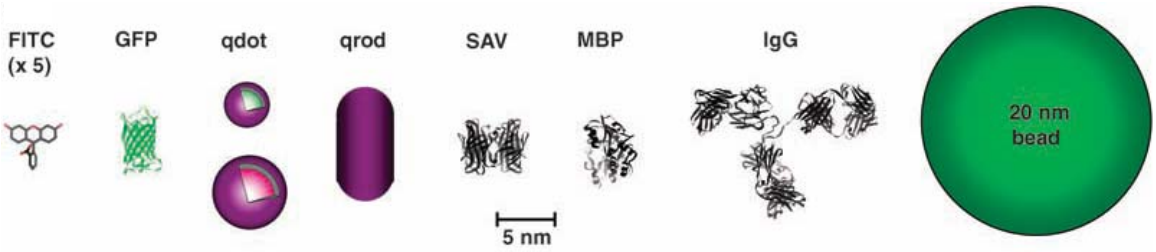

(Michalet *et al*., 2005)

Figure 2.2. Size comparison of QDs and comparable objects. FITC, fluorescein isothiocyanate; GFP, green fluorescent protein; qdot, green (4 nm, top) and red (6.5 nm, bottom) CdSe/ZnS qdot; qrod, rod-shaped qdot (size from Quantum Dot Corp.'s Web site). Three proteins—streptavidin (SAV), maltose binding protein (MBP), and immunoglobulin G (IgG).

2.1.2. Optical Properties. QDs have some unique optical properties, which make them to be a much better imaging tool for delivering and monitoring biomolecules into living cells.

2.1.2.1. Quantum dots have composition- and size-dependent absorption and emission. QDs exhibit discrete size-dependent energy levels. As the size of the QDs increases, the energy gap also increases, yielding a size-dependent rainbow of colors. The color of QDs can be tunable, from ultraviolet to infrared, via varying the size and the composition of QDs (Alivisatos *et al*., 2005; Michalet *et al*., 2005) (Figure 2.3).

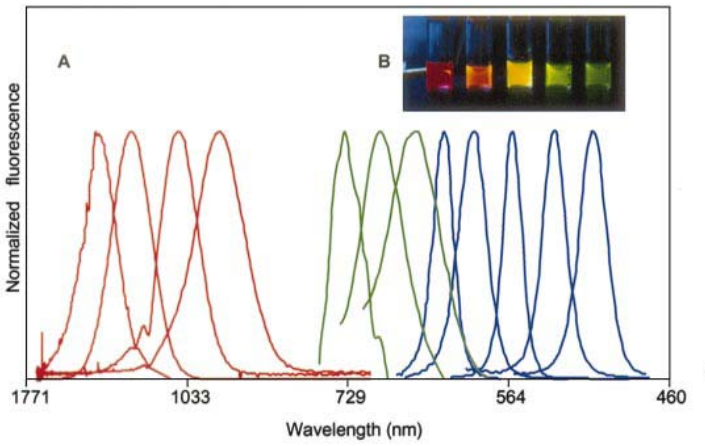

(Bruchez *et al*., 1998)

Figure 2.3. Composition- and size-dependent absorption and emission. (A) Size- and material-dependent emission spectra of several surfactant-coated semiconductor nanocrystals in a variety of sizes. The blue series represents different sizes of CdSe nanocrystals with diameters of 2.1, 2.4, 3.1, 3.6, and 4.6 nm (from right to left). The green series is of InP nanocrystals with diameters of 3.0, 3.5, and 4.6 nm. The red series is of InAs nanocrystals with diameters of 2.8, 3.6, 4.6, and 6.0 nm. (B) A true-color image of a series of silica-coated core (CdSe)-shell (ZnS or CdS) nanocrystal probes in aqueous buffer, all illuminated simultaneously with a handheld ultraviolet lamp.

2.1.2.2. Unique optical spectra. Organic dyes typically have narrow absorption spectra, which makes simultaneous excitation difficult in most cases. Furthermore, they have asymmetric emission spectra broadened by a red-tail, making quantitation of different probes difficult. In contrast, QDs have broad absorption spectra, enabling excitation by a wide range of wavelengths, and their emission spectra are symmetric and narrow (Figure 2.4.) (Alivisatos *et al*., 2005; Michalet *et al*., 2005). Consequently, QDs can be excited with a single wavelength of light, resulting in multicolor that may be detected simultaneously.

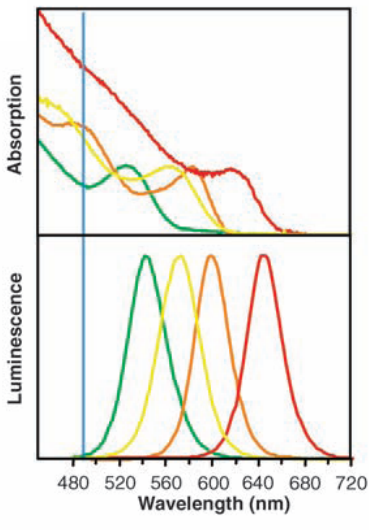

(Michalet *et al*., 2005)

Figure 2.4. Absorption and emission spectra of QDs. Absorption (upper curves) and emission (lower curves) spectra of four CdSe/ZnS QD samples. The blue vertical line indicates the 488-nm line of an argon-ion laser, which can be used to efficiently excite all four types of QDs simultaneously.

2.1.2.3. Photostability. QDs have strong photostability due to their inorganic composition, making them extremely resistant to photobleaching compared to organic dyes (Figure 2.5.). This characteristic makes QDs very attractive probes for continuous monitoring of biological phenomena.

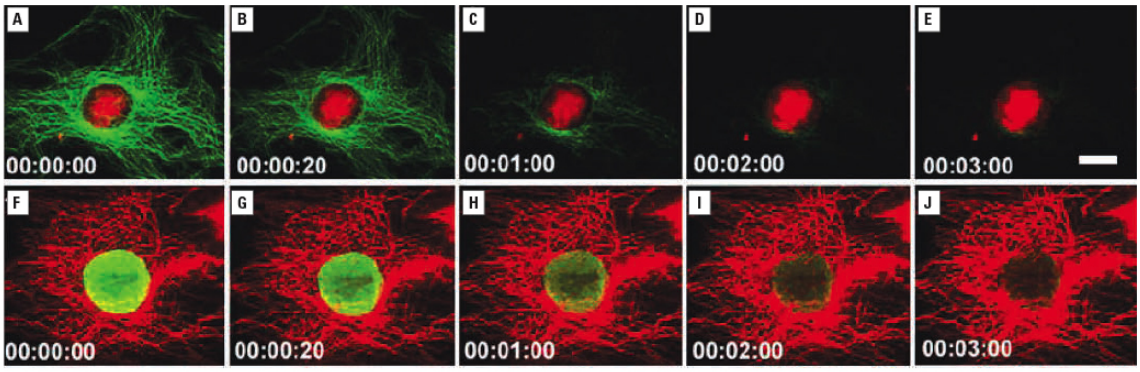

(Wu *et al*., 2003)

Figure 2.5. Photostability comparison between QDs and Alexa 488. Top row: nuclear antigens were labeled with QD 630-streptavidin (red), and microtubules were labeled with Alexa 488 conjugated to anti-mouse IgG (green) simultaneously in a 3T3 cell. Bottom row: microtubules were labeled with QD 630-streptavidin (red), and nuclear antigens were stained green with Alexa 488 conjugated to anti-human IgG.

2.1.2.4. Long luminescent lifetimes. Typically, the luminescent lifetimes of organic dyes or auto-fluorescent proteins are a few nanoseconds. In contrast, the lifetime of QDs is 10 to 40 ns (Alivisatos *et al*., 2005), which is significantly longer than organic dyes. Such long lifetime greatly reduced background noises in live cell imaging. Common organic dyes allow singlet–singlet electronic transition in a few nanoseconds. Unfortunately, this prompt emission coincides with a high degree of short-lived autofluorescence background from many naturally occurring species in a biological specimen. Delayed (longlifetime) fluorescence labels for time-gated image and fluorescence lifetime imaging have long been sought for enhanced contrast in cellular imaging. However, because their fluorescence lifetime is too long, these probes have a limited photon turnover rate and therefore limited sensitivity. QDs emits light slowly enough that most of the autofluorescence background is over by the time emission occurs but fast enough to maintain a high photon turnover rate. Therefore QDs may be ideal

probes for spectrally multiplexed, time-gated cellular detection with enhanced selectivity and sensitivity (Dahan *et al*., 2001).

2.1.3. Biological Applications. The first advantage of QDs is their utility as a stable fluorescent marker for many purposes, including cancer diagnosis and treatment. Wu *et al*. used QDs linked to streptavidin and antibody to detect the receptor Her2 on SK-BR-3 breast cancer cells (Wu *et al*., 2003). Type II QDs emit light within the NIR spectrum and have a potential surgical utility by providing optical guidance that can result in reduction of cancer metastases (Soltesz *et al*., 2006). QD fluorescence can also be used for sentinel lymph node (SLN) mapping and removal, which provides accurate staging and therapeutic planning (Kim *et al*., 2004; Parungo *et al*., 2005a; Parungo *et al*., 2005b; Soltesz *et al*., 2005; Soltesz *et al*., 2006). QDs properties such as multiplexing potential, photostability, and inorganic nature make them useful for drug discovery. For example, they allow monitoring of multiple drug candidates over extended time periods in cell culture simultaneously, thus saving time and cost (Ozkan, 2004). Lai *et al*. used surface-modified CdS QDs as chemically removable caps to retain drug molecules and neurotransmitters inside mesoporous silica nanospheres. The CdS cap ensures the drug is inside the system until released by disulfide bond reducing reagents (Lai *et al*., 2003; Alivisatos *et al*., 2005).

2.2. INTRODUCTION OF CPPs

CPPs are peptides made of less than 30 amino acids. These CPPs are rich in arginine and lysine residues. Positively charged amino acids, hydrophobicity and amphipathicity are common features shared among many of the known CPPs.

The three most widely studied CPPs are from the human immunodeficiency virus type 1 (HIV-1) transcriptional activator Tat protein (Frankel and Pabo, 1988; Green and Loewenstein, 1988), the Drosophila homeodomain transcription factor antennapedia (Joliot *et al*., 1991), and the herpes simplex virus structural protein VP22 (Elliott and O'Hare, 1997). Derived from HIV Tat peptide, many basic peptides have been generated, such as Polyarginines, Pep-1, MPG, pVEC, SAP . These peptides and their variations can covalently cross-link or noncovalently interact with a wide variety of biologically active molecules up to 200 nm in diameter (Wadia and Dowdy, 2002).

Due to their low cytotoxicity and ability to carry multiple types of cargo, CPPs have been used to improve delivery of many molecules such as small molecules, oligonucleotide, plasmid DNA, peptide, protein, nanoparticle, lipid-based formulation, virus, quantum dots. The number of applications using CPPs is consistantly increasing, and so far more than 300 studies using either covalent or non-covalent CPP-based strategies from in vitro to in vivo have been reported (Heitz *et al*., 2009).

2.3. INTRODUCTION OF ENDOCYTOSIS

Endocytosis is a basic cellular process that is used by cells to internalize a variety of molecules. Endocytosis is the process of internalization of PM, ligands and fluid into the cell, which can be divided into two main categories: phagocytosis or pinocytosis. Phagocytosis takes place only in professional phagocytes such as macrophages, monocytes and neutrophils, while pinocytosis occurs in most mammalian cell types (Gong *et al*., 2008). Therefore, pinocytosis is called generally endocytosis, which can be categorized into four different types: macropinocytosis, clathrin-dependent endocytosis,

caveolae-dependent endocytosis or clathrin- and caveolae-independent endocytosis (Conner and Schmid, 2003; Mayor and Pagano, 2007; Gong *et al*., 2008) (Figure 2.6.).

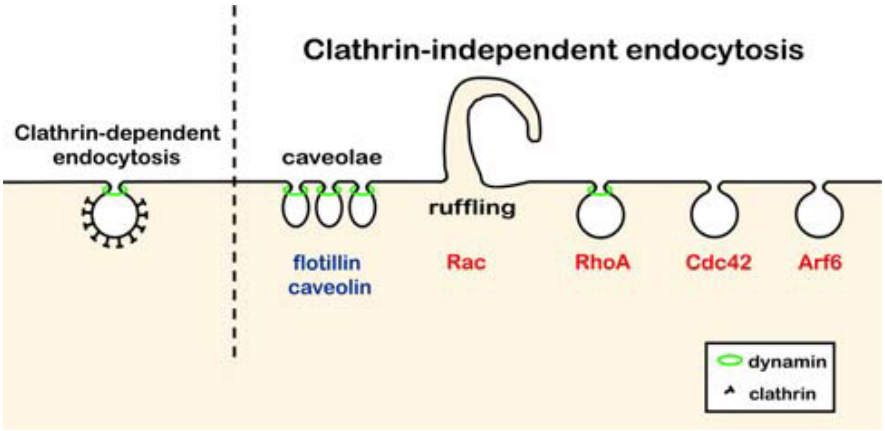

(Sandvig *et al*., 2008)

Figure 2.6. Overview of different types of endocytosis.

2.3.1. Clathrin-dependent Pathway. Clathrin-dependent pathway is the major and best characterized endocytic pathway. Clathrin has specific trafficking motifs, including the tyrosine-based motif, di-leucine-based motif, NPXY and mono-/multi-ubiquitination (Mousavi *et al*., 2004). These trafficking motifs are recognized by various adaptor proteins, most notably the adaptor protein 2 (AP-2) (Gong *et al*., 2008). During internalization, the adaptor proteins link the membrane cargo proteins to clathrin, concentrating them in clathrin-coated pits. The clathrin-coated pits invaginate into the cytoplasm, and eventually pinch off from the plasma membrane to form clathrin-coated vesicles (80–120 nm in diameter) (Conner and Schmid, 2003).

The clathrin-dependent pathway is a highly regulated process. The assembly of the clathrin lattice on the membrane is essential for the detachment of the vesicles. Drugs that

dissociate clathrin and adaptor protein complex from membrane can inhibit this pathway. The small GTPase dynamin is also very important for clathrin-dependent endocytosis because it is required to facilitate the fission process (Damke *et al*., 1994). Therefore, clathrin-dependent endocytosis requires energy.

2.3.2. Caveolea-dependent Pathway. Caveolae are a special type of lipid rafts. Caveolea have a unique morphology of flask-shaped invaginations (50–80 nm in diameter) on the cell surface (Conner and Schmid, 2003).

2.3.2.1. Caveolin-dependent endocytosis. Caveolae contain a high level of caveolin proteins, including three caveolin isoforms: caveolin-1, caveolin-2, and caveolin-3. Caveolin-1 and caveolin-2 are mainly found in non-muscle cells, while caveolin-3 is expressed in skeletal and smooth muscle cells (Parton and Simons, 2007). Cholesterol is required for caveolar uptake and drugs that bind to or sequester cholesterol perturb internalization of caveolea (Schnitzer *et al*., 1994). Caveolar budding requires Src-family kinases, dynamin and local actin polymerization (Sverdlov *et al*., 2007).

2.3.2.2. Flotillin-dependent endocytosis. Recent report shows that an alternative caveolin-independent mechanism for making caveolae can somehow cause the formation of caveolae. Flotillin 1 and flotillin 2 have similar topology to caveolin 1. Overexpression of flotillin 1 and flotillin 2 in HeLa cells induced membrane curvatures and formation of membrane invaginations morphologically similar to caveolae (Frick *et al*., 2007). These flotillin-positive but caveolin-negative structures might be internalized by “classical” caveolae (Frick *et al*., 2007; Hansen and Nichols, 2009).

2.3.3. Macropinocytosis. Macropinocytosis refers to the formation of large endocytic vesicles of irregular size and shape, generated by actin-driven envagination of

the plasma membrane (Swanson and Watts, 1995). A ruffle is formed by a liner band of outward-directed actin polymerization near the plasma membrane. The endocytic vesicles of macropinocytosis pathway, also known as macropinosomes, are formed through the folding back and closure of membrane ruffle structures. Macropinosomes have no coat and do not concentrate receptors. Macropinosomes are large vesicles with range from 1 to 5 μm in diameter (Conner and Schmid, 2003).

Ruffling is dependent on actin cytoskeleton. Therefore, drugs that disrupt the actin cytoskeleton can inhibit macropinocytosis. The ruffling response is also dependent on protein kinase C. Macropinocytosis can also be inhibited by amiloride and its analogs, which inhibit the Na^+/H^+ exchange protein in the plasma membrane. Recent studies show that macropinocytoiss is lipid-raft dependent process. Therefore, cholesterol depletion can inhibit macropinocytosis.

2.3.4. Clathrin- and Caveolea-independent Pathways. The research on clathrin- and cavoelea-independent endocytosis is still at an early stage. So far, there is still no a satisfactory classification for those novel pathways. Recently, Mayor and Pagano proposed two different classifications. According to the requirement of dynamin, these pathways are divided into dynamin-dependent and dynamin-independent mechanism. A second division is related to the involvement of small GTPases. Four different types are subdivided by RhoA-regulated, cdc42-regulated, and Arf6-regulated endocytic pathway (Mayor and Pagano, 2007) (Figure 2.6).

3. MATERIAL AND METHODS

3.1. QUANTUM DOTS

CdSe/ZnS quantum dots (Adirondack Green, 520nm) were purchased from Evident Technologies (Troy, NK, USA). These quantum dots have a PEG lipid surface coated with carboxyl terminal groups. The emission and excitation peak wavelengths are 520 nm and 505 nm respectively. The hydrodynamic diameter is 25 nm.

3.2. NONA-ARGININES (sR9)

Nona-arginines were synthesized by solid-phase peptide synthesis (Sigma-Aldrich, Saint Louis, MO, USA). The synthesized peptides were purified by high performance liquid chromatography (HPLC) using a reverse column. The purity of sR9 was up to 99%.

3.3. CHEMICALS

Fetal bovine serum, Ham's F-12 medium with L-glutamine, trypsin-EDTA (1x), Penicillin-streptomycin, sucrose, sodium azide, sodium fluoride, and chlorpromazine were purchased from Fisher Scientific (Pittsburgh, PA, USA). Nystatin, filipin, 5-(N-ethyl-N-isopropyl) amirolide (EIPA), Cytochalasin D (Cyt D), antimycin A, and monodansylcadaverine (MDC) were obtained from Sigma-Aldrich.

3.4. CELL CULTURE

The human bronchoalveolar carcinoma-derived cell line (A549) was purchased from ATCC (Manassas, VA, USA). Cells were maintained in Ham's F-12 medium supplemented with 10% fetal bovine serum, 100 units/mL penicillin, 100 μg/mL

streptomycin, and grown at 37ºC in a 5% CO_2 humidified environment. A549 cells were seeded into 35 mm glass-bottom tissue culture plates (MatTek, Ashland, MA, USA) at an initial confluency of 20%, and allowed to attach for 48 hours.

3.5. GEL RETARDATION ASSAY

The QD and sR9 complexes were prepared at different molecular ratios (1:10, 1:20, 1:30 and 1:60) and incubated for 20 min at room temperature to form noncovalent binding between sR9 and QDs. These complexes were analyzed by electrophoresis in a 0.6% agarose gel in 0.5% TAE buffer at 130 voltages for 60 min. The gel was visualized by UV light.

3.6. QD UPTAKE WITH sR9 AT DIFFERENT MOLECULAR RATIOS

To determine the optimal ratio between QD and sR9 for efficient delivery, A549 cells were incubated with QD/sR9 at different molecular ratios (1:10 to 1:60). The cells were washed with ice-cold PBS for six times to remove unbound QD/sR9. Then fluorescent image and quantitation were performed.

3.7. CYTOTOXICITY MEASURMENT

To determine the cytotoxicity of QD/sR9, A549 cells were treated with 12.5, 25, 50, 100, and 200 nM of QDs for 24 hours. Untreated cells served as a control group. The MTS assay (Cell Titer 96® Aqueous One Solution Assay, Promega) was used to determine cytotoxicity. Absorbance was measured at 490 nm using a microplate reader (FLOURstat; BMG Labtechnonogies, Durham, NC, USA).

3.8. QUANTUM DOTS AND sR9 NONCOVALENT BINDING AND INTERNALIZATION

QDs were pre-mixed with sR9 peptides at the molecular ratio of 1:20 at room temperature for 20 min. Immediately upon removal of medium from A549 cells, the cells were treated with the QD/sR9 mixture at a final concentration of 150 nM for QDs for designated period of time. After treatment, cells were washed with ice-cold PBS for six times. Phenol red free medium (2 mL) (Invitrogen, Carlsbad, CA, USA) was added for fluorescent image study.

3.9. UPTAKE STUDIES

To determine the mechanism of uptake, specific inhibitors of each type of uptake pathway were selected. Table 4.1 lists all the inhibitors in our internalization studies.

3.9.1. Energy Inhibition. To determine whether uptake of QD/sR9 was energy-dependent, cells were incubated with QD/sR9 under varying metabolic conditions. For low temperature studies, cells were treated at either 37ºC or 4ºC. For low temperature group, cells were preincubated at 4ºC for 30min, and then cells were treated with QD/sR9 at 4ºC for another 1 hour. Treatment at 37°C was used as the control group. In metabolic inhibition experiments, cells were incubated in the absence or presence of a mixture of metabolic inhibitors (0.15% sodium azide, 15 mM sodium fluoride, and 2 μg/mL antimycin A). Cells were pretreated with a mixture of metabolic inhibitors for 1 hour followed by addition of QD/sR9 to the cells and then incubated for another 1 hour.

Table 4.1. Inhibitors for mechanistic studies on cellular uptake

Inhibitor	Effect	Mechanism	References
Low temperature	General inhibitor of endocytosis	Energy depletion	Vives, Brodin *et al*. 1997; Kaplan, Wadia *et al*. 2005
Metabolic inhibitors	General inhibitor of endocytosis	Energy depletion	Almofti, Harashima *et al*. 2003; Khalil, Kogure *et al*. 2006
Chlorpromazine	Inhibitor of clathrin-dependent endocytosis	Relocates clathrin and adaptor protein complex 2 (AP2)	Wang, Rothberg *et al*. 1993; Yao, Ehrlich *et al*. 2002
MDC	Inhibitor of clathrin-dependent endocytosis	Stabilization of nascent clathrin-coated vesicles	Phonphok and Rosenthal 1991; Panicker, Buhusi *et al*. 2006
Hypertonic medium	Inhibitor of clathrin-dependent endocytosis	Dissociation of clathrin lattice	Hansen, Sandvig *et al*. 1993
Filipin	Inhibitor of lipid-raft/caveolae	Cholesterol binding	Schnitzer, Oh *et al*. 1994; Khalil, Kogure *et al*. 2006
Nystatin	Inhibitor of lipid-raft/caveolae	Sequester cholesterol	Wadia, Stan *et al*. 2004
EIPA	Specific inhibitor of macropinocytosis	Inhibits the Na+/H+ exchange protein	Hewlett, Prescott *et al*. 1994
Cyt D	Inhibitor of macropinocytosis	F-actin depolymerization	Cooper 1987; Wadia, Stan *et al*. 2004

3.9.2. Clathrin-dependant Pathway Inhibition. To disrupt clathrin-dependent endocytosis, hypertonic challenge, chlorpromazine, and MDC were used. Cells were

pretreated with 0.45 M sucrose, 10 μM chlorpromazine, or 25 μg/mL MDC, respectively, for 30 min, and then QD/sR9 were added to the cells followed by 1 hour incubation.

3.9.3. Caveolea-dependant Pathway Inhibition. To inhibit caveolea-dependent endocytosis, filipin and nystatin were used to deplete cholesterol. Cells were preincubated with 3 μg/mL filipin and 20 μg/mL nystatin, respectively, for 30 min before treatment with QD/sR9 for another 1 hour.

3.9.4. Macropinocytosis Pathway Inhibition. EIPA (30 μM) or Cyt D (1 μg/mL) was selected to block macropinocytosis. Cells were pretreated with these inhibitors for 30 min before treatment with QD/sR9 for another 1 hour.

3.9.5. siRNA Transfection. Due to potential nonspecific effects and toxicity of inhibitors, clathrin heavy chain and caveolin-1 siRNA (Sigma-Aldrich) were used to knockdown clathrin and caveolar pathways. The sense and antisense sequences of these siRNA are as follows.

Clathrin HC: 5'-CCCUAAACACCUCAACGAU-3' (sense)
5'-AUCGUUGAGGUGUUUAGGG-3' (antisense)

Caveolin-1 5'-CAUUAUGACCGGGCUCAUA-3' (sense)
5'-UAUGAGCCCGGUCAUAAUG-3' (antisense)

Transfection of siRNA into the A549 cells were performed at a ~30% cell confluence. siRNA was complexed with Lipofectamine 2000 reagent according to the manufacturer's instructions (Invitrogen). Western blot and QD/sR9 uptake studies were conducted 3 days after transfection.

3.10. WESTERN BLOT ANALYSIS

A549 cells were lysed in Lysis buffer (150 mM sodium chloride, 1.0% Triton X-100, 50 mM Tris, pH 8.0) containing 1% protease inhibitor cocktail (Sigma-Aldrich). The protein concentration was quantified by the Bradford procedure (BioRad, Hercules, CA, USA). Ten μg total cell protein was electrophoresed on 8% (clathrin-heavy chain) or 12% (caveolin-1) SDS-PAGE, followed by electrotransferring to a nitrocellulose membrane. Clathrin-heavy chain was detected using a mouse monoclonal antibody at a dilution of 1:200 and goat anti-mouse IgG-HRP secondary antibody (Santa Cruz, CA, USA). Caveolin-1 protein was detected using a rabbit monoclonal antibody at a dilution of 1:1000 and goat anti-rabbit IgG-HRP secondary antibody (Cell Signaling, Danvers, MA, USA). The blots were probed with the ECL Western blot detection system according to the manufacturer's instructions (Thermo Fisher Scientific, Rockford, IL, USA).

3.11. EPIFLUORESCENT MICROSCOPY

After treatment with QD/sR9, cells were viewed under the Olympus IX51 inverted microscope at 600X total magnification using a UPLFLN 60X NA 1.25 objective (Olympus, Center Valley, PA, USA). QD filter set (EX 435/40, EM 519-700) was used for QDs (Semrock). Images were captured with a Hamamatsu ORCA285 CCD camera. Z series images of entire cell volume were taken at 0.3 μm internals. Images were analyzed by the SlideBook software (Intelligent Imaging Innovations, Denver, CO, USA).

3.12. STATISTICAL ANALYSES

Data of fluorescent images were representatives of at least two independent experiments. Fluorescent intensity was quantified by using the SlideBook software. Data represented mean fluorescence intensity (after background subtraction) of a single plane in Z series. One-tailed unpaired Student's t-test was used for significance testing, using *p* values of 0.01 and 0.05. Data were expressed as the mean ± standard deviation from 10 different fields performed in two independent experiments.

4. RESULTS

4.1. FORMATION OF QD/sR9 NONCOVALENT BINDING

To test whether sR9 peptide could noncovalently bind to QDs, QDs were mixed with sR9 at various molecular ratios (1:10, 1:20, 1:30 and 1:60). These mixtures were separated by electrophoresis in a 0.6% agarose gel (Figure 4.1). The QD mobility was reduced as the amount of sR9 increased. This result indicated that sR9 peptide interacted with QDs and bound non-covalently.

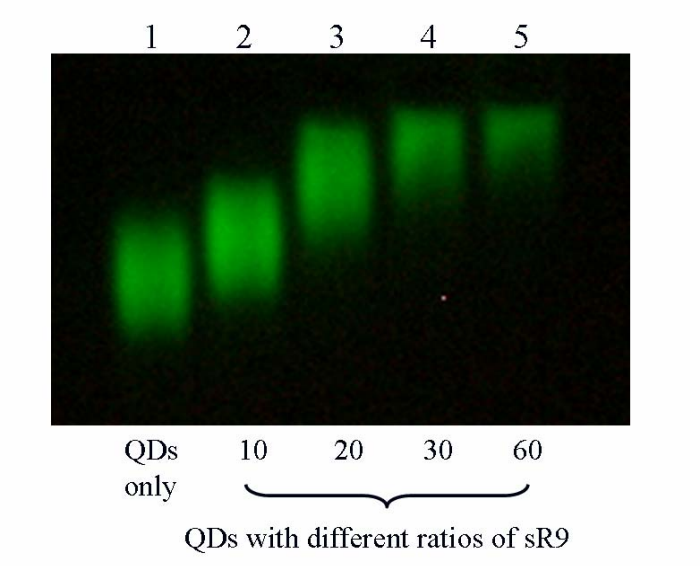

Figure 4.1. Gel retardation analysis of the interaction between QDs and sR9. QDs were pre-mixed with sR9 at different molecular ratios. Lane 1 showed QDs without sR9, while Lanes 2-5 represented QDs mixed sR9 at ratios of 10, 20, 30 and 60 respectively. The mobility was reduced as the amount of sR9 increased.

4.2. MOLECULAR RATIOS BETWEEN QD AND sR9 AFFECT UPTAKE

To determine the optimal ratio for cellular uptake, A549 cells were incubated with QDs (150 nM) preincubated at different molecular ratios with sR9. Figure 4.2 shows that

at ratio from 1:10 to 1:30, QD uptake was increased as the ratio of sR9 increased. However, when the ratio was above 1: 30, the speed of internalization reached saturation. In subsequent studies, we selected 1:20 as interaction ratio between QDs and sR9, because this ratio provides good imaging quality.

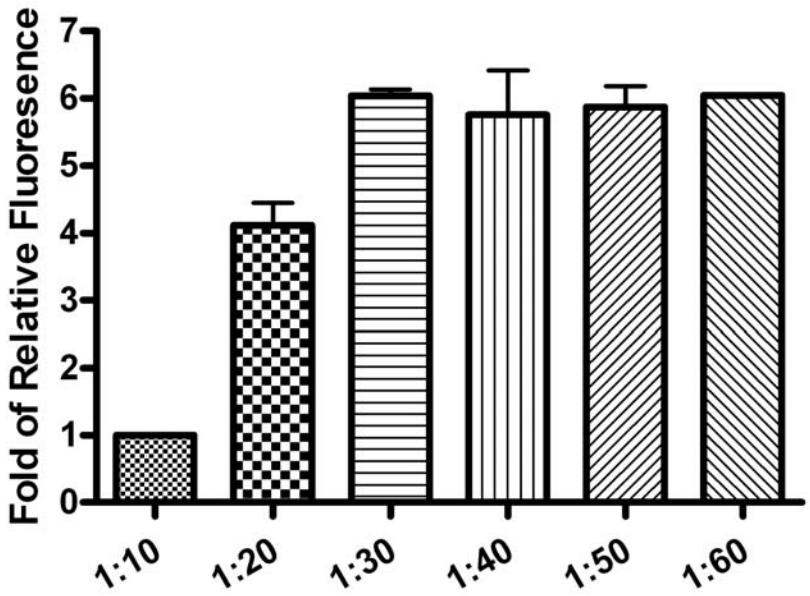

Figure 4.2. QD uptake with sR9 at different molecular ratios. QDs were pre-mixed with sR9 at molecular ratios (1:10 to 1:60). A549 cells were treated with QD/sR9. Error bars represent the S.D. for 10 different fields performed in two independent experiments. Fluorescence intensity is normalized relative to 1:10.

4.3. TIME DEPENDENT UPTAKE

To determine the optimal dosing time, A549 cells were incubated with QD/sR9 for 5 min, 20 min, 40 min, 1 hour and 3 hours. Figure 4.3 shows that the uptake of QD/sR9

was dramatically increased after 20 min. At 1 hour, the uptake reached to the peak. Since internalization was high at 1 hour, this time point was used for further experiments.

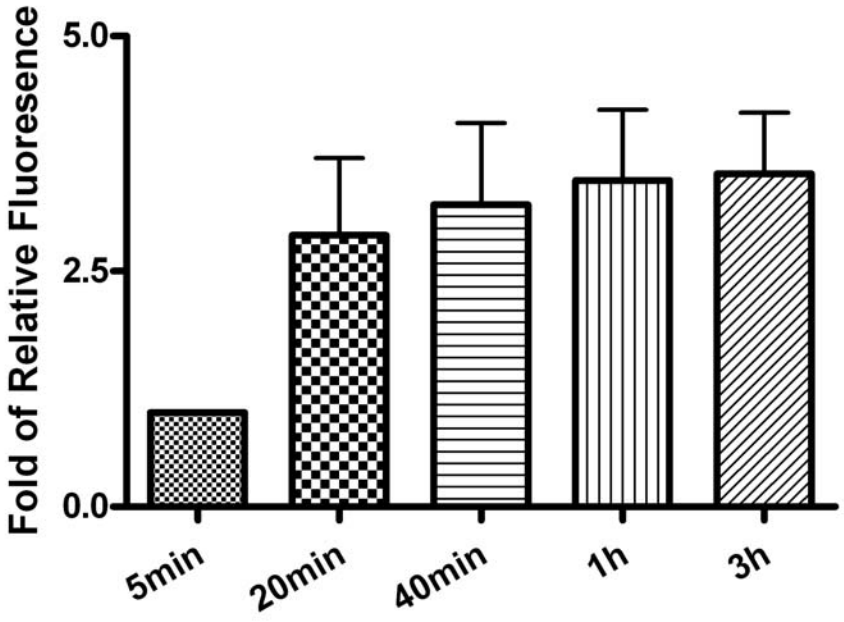

Figure 4.3. Time dependent uptake of QD/sR9. QDs were pre-mixed with sR9 at molecular ratios (1:20). A549 cells were treated with QD/sR9 for 5 min, 20 min, 40 min, 1 hour and 3 hour, respectively. Error bars represent the S.D. for 10 different fields performed in two independent experiments. Fluorescence intensity is normalized relative to 5 min.

4.4. CYTOTOXICITY OF QD/sR9

To assess potential cytotoxicity caused by QD/sR9 complex, A549 cells were treated with QD/sR9 (1:20) complex at various QD concentrations for 24 hours. No cytotoxicity of QD/sR9 was observed at concentrations tested up to 200 nM (Figure 4.4).

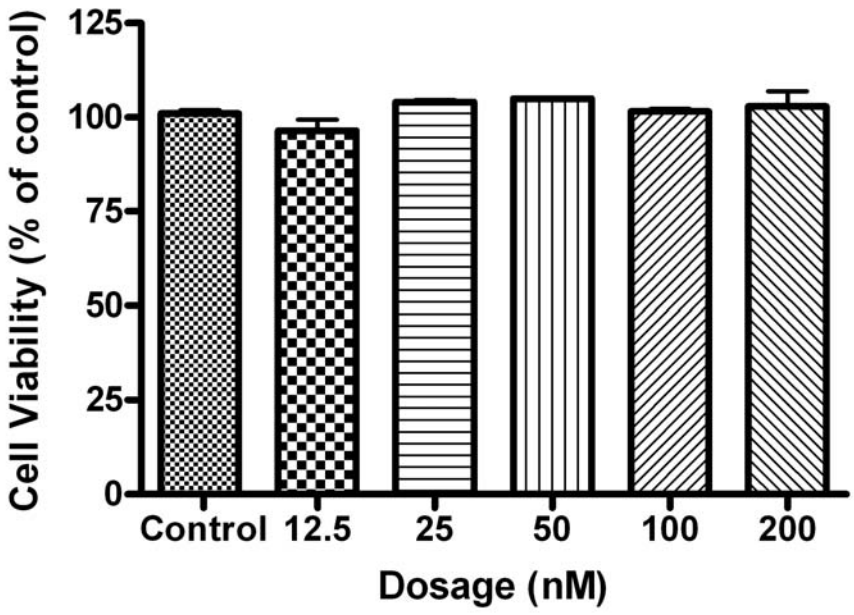

Figure 4.4. Cell viability of QD/sR9 treated cells. A549 cells were treated with QD/sR9 (1:20) for 24 hours. The concentrations of QDs used were: 12.5, 25, 50, 100 and 200 nM. The cells treated with QD/sR9 showed a statistically insignificant difference from the control group.

4.5. CELLULAR UPTAKE OF QDs FACILITATED BY sR9 PEPTIDE

To determine the ability of sR9 peptide to facilitate QD delivery, A549 cells were treated with 150 nM QDs alone or 150 nM QDs premixed with sR9 at a ratio of 1:20. After incubation of 5 min, 20 min, 40 min and 60 min, QDs treated cells were observed under epifluorescence microscope. Figure 4.5 shows that the uptake of QD/sR9 was statistical significantly increased above QDs alone at all time points. Uptake of the QD/sR9 complex was extremely rapid, beginning at 5 min.

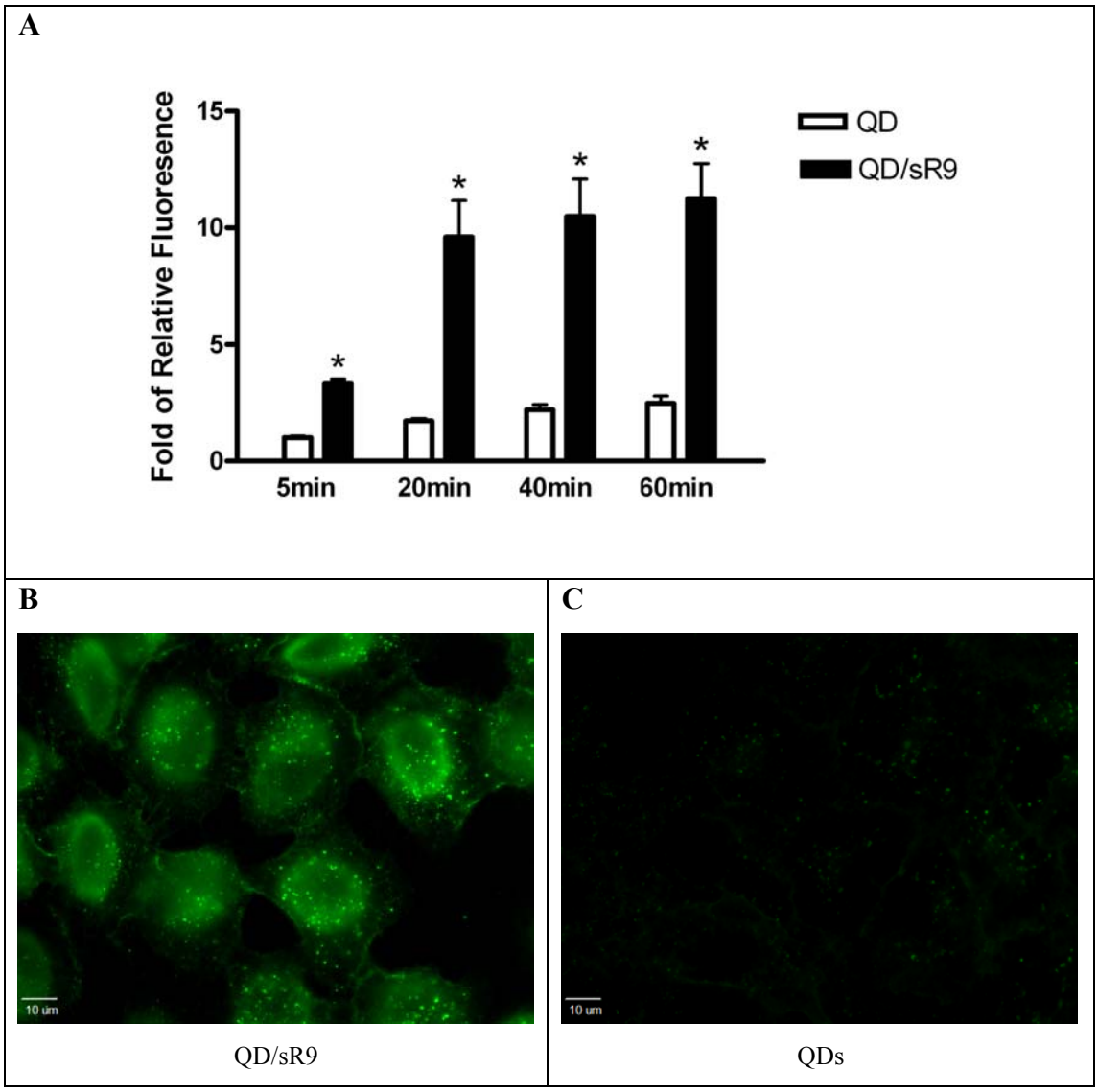

Figure 4.5. sR9 facilitate QD uptake. A: the relative fluorescence intensity of QDs. A549 cells were treated with 150 nM QD and 150 nM QD/sR9 (1:20) for 5 min, 20 min, 40 min and 60 min respectively. Error bars represent the S.D. for 10 different fields performed in two independent experiments. Significance indicated by: $*p < 0.01$ vs. QD alone group. Fluorescence intensity is normalized relative to QD alone at 5 min. B and C: the images of QDs' uptake with and without sR9 after 1 hour treatment. Images represent single plane of Z series.

4.6. MECHANISM OF QD/sR9 INTERNALIZATION

Endocytosis, an essential cellular process of internalizing extracellular materials, utilizes several distinct pathways. To determine the mechanism of sR9-mediated QD delivery, a series of inhibition studies were carried out.

4.6.1. Energy Dependent Studies. To understand whether uptake of QD/sR9 was mediated by energy-dependent endocytosis, we used low temperature or a mixture of metabolic inhibitors to deplete intracellular energy. For the low temperature study, the cells were incubated with QD/sR9 at 37°C and 4°C respectively. As shown in Figure 4.6b, QD/sR9 internalization at 4°C was significantly impeded. Compared to 37°C, the fluorescence intensity at 4°C decreased by 72% (p's < 0.01). In the metabolic inhibition study, A549 cells were incubated with QD/sR9 in the presence or absence of a mixture of metabolic inhibitors (0.15% sodium azide, 15mM sodium fluoride, and 2μg/ml antimycin A). As shown in Figure 4.6c, these metabolic inhibitors strongly inhibited the uptake of QD/sR9. In comparison with the control group, the fluorescent intensity in the presence of metabolic inhibitors decreased by 59% (p's < 0.01) (Figure 4.6d).

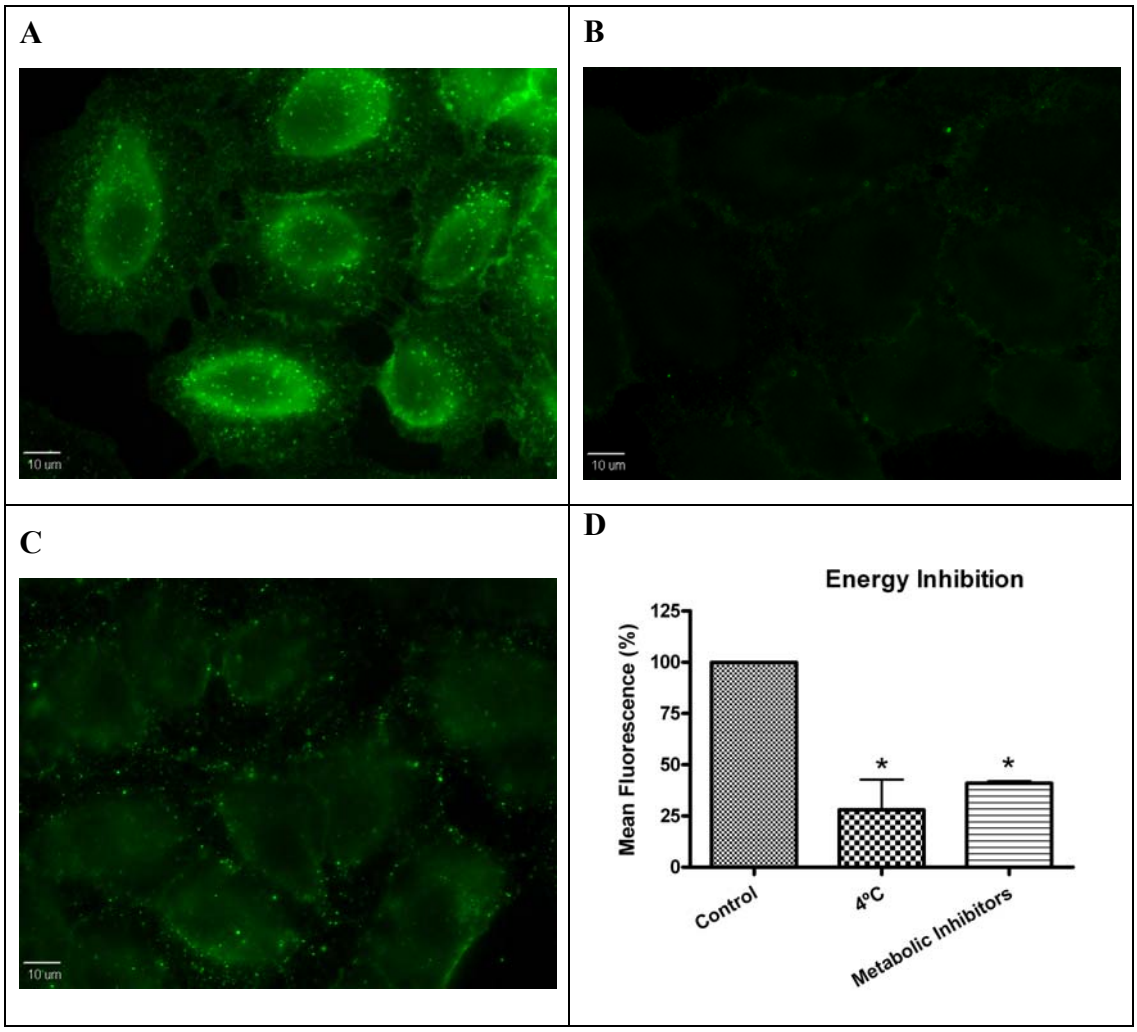

Figure 4.6. Energy inhibition reduced QD/sR9 internalization. A: the images of control cells. B: the images of cells pre-treated at 4°C for 30 min, then incubated with QD/sR9 for additional 1 hour. C: the images of cells pre-treated with metabolic inhibitor mixture for 1 hour, then incubated with QD/sR9 for additional 1 hour. Images represent single plane of Z series. D: mean fluorescence intensity. Error bars represent the S.D. for 10 different fields performed in two independent experiments. Significance indicated by: *$p < 0.01$ vs. control.

4.6.2. Clathrin-dependent Pathway. To perturb the clathin-dependent uptake pathway, three methods were used: MDC, hyperotonic sucrose, and chlorpromazine. The inhibitory activity of MDC is attributed to the stabilization of nascent clathrin-coated vesicles, which limit new clathrin-coated vesicle production (Phonphok and Rosenthal, 1991). The underlying mechanism of hypertonic sucrose involves the dispersion of clathrin lattices on the plasma membrane (Hansen *et al*., 1993). Chlorpromazine is a cationic amphipathic drug that relocates clathrin and adaptor protein complex 2 (AP2) from plasma membrane to endosomal membrane (Wang *et al*., 1993). MDC reduced the uptake of QD/sR9 by 45% while hypertonic medium decreased uptake by 59% (data not shown). Contrarily, chlorpromazine did not result in significant uptake reduction compared to the control group (Figure 4.7).

4.6.3. Lipid-raft/Caveolea-dependent Pathway. Nystatin and filipin, lipid raft inhibitors, are used to block caveolea-dependent endocytic pathway (Schnitzer *et al*., 1994; Wadia *et al*., 2004). Treatment of cells with these two inhibitors moderately reduced the QD/sR9 internalization by 36% and 35%, respectively (Figure 4.8) indicating that a lipid raft-dependent process was involved in QD/sR9 internalization.

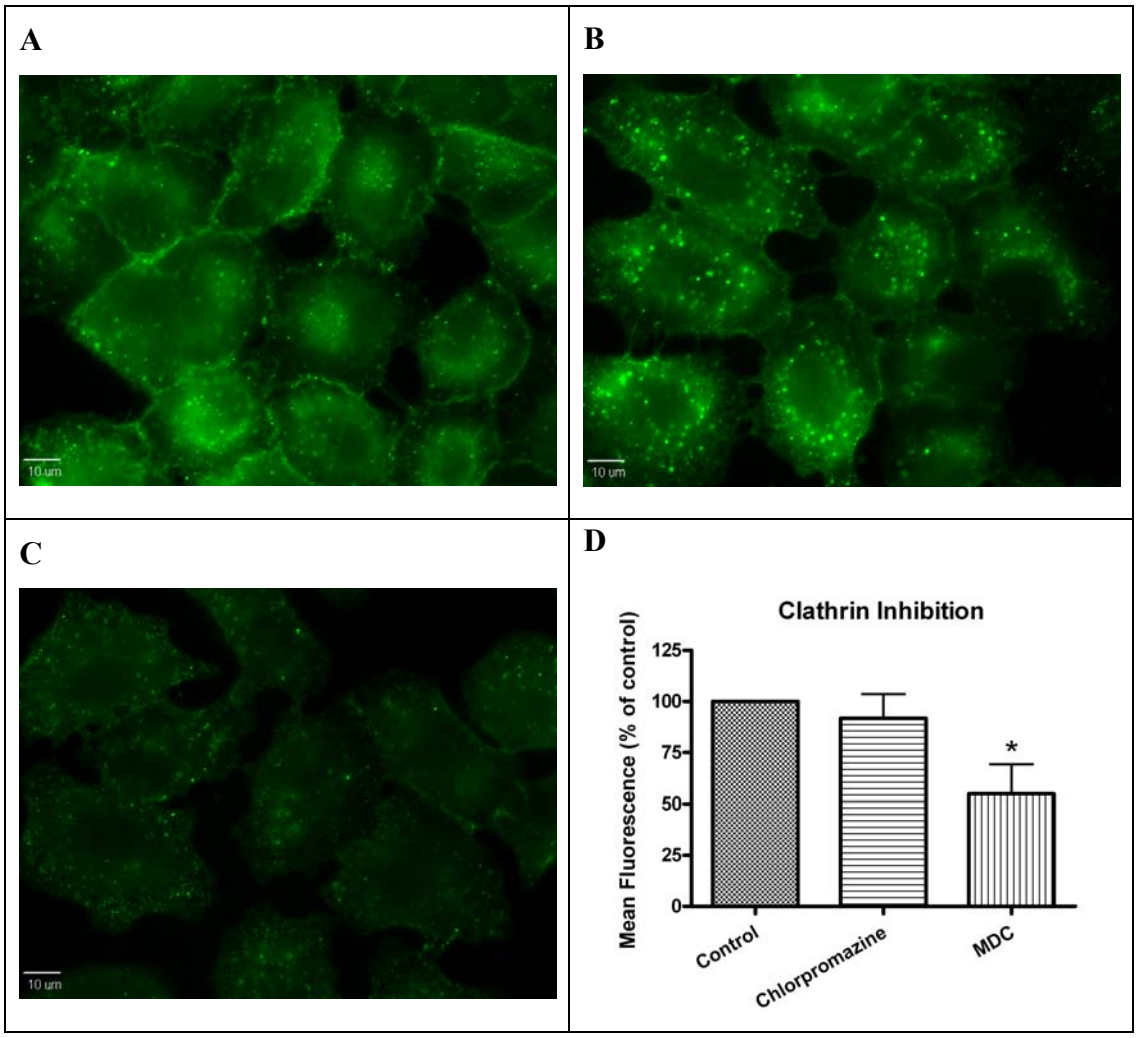

Figure 4.7. Two different clathrin inhibitors produced different effects on QD/sR9 internalization. A: the images of control cells. B: the images of cells pre-treated with chlorpromazine for 30 min, then incubated with QD/sR9 for additional 1 hour. C: the images of cells pre-treated with MDC for 30 min, then incubated with QD/sR9 for additional 1 hour. Images represent single plane of Z series. D: mean fluorescence intensity. Error bars represent the S.D. for 10 different fields performed in two independent experiments. Significance indicated by: $*p < 0.01$ vs. control.

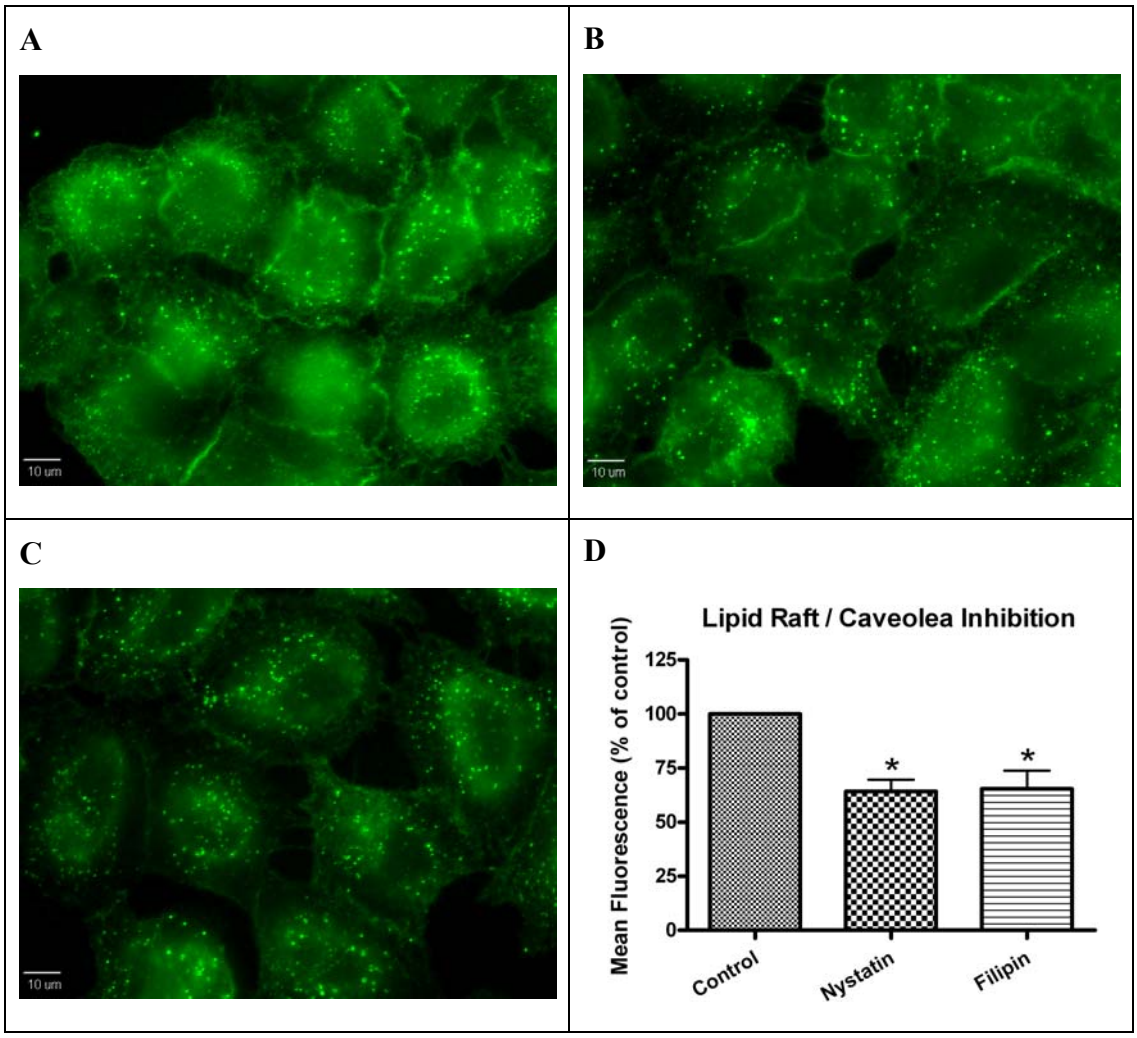

Figure 4.8. Lipid raft/Caveolea inhibition decreased QD/sR9 internalization. A: the images of control cells. B: the images of cells pre-treated with nystatin for 30 min, then incubated with QD/sR9 for additional 1 hour. C: the images of cells pre-treated with filipin for 30 min, then incubated with QD/sR9 for additional 1 hour. Images represent single plane of Z series. D: mean fluorescence intensity. Error bars represent the S.D. for 10 different fields performed in two independent experiments. Significance indicated by: *$p < 0.01$ vs. control.

4.6.4. Macropinocytosis Pathway. EIPA is an inhibitor of Na^+/H^+ exchange required for macropinocytosis (Hewlett *et al*., 1994). Cytochalasin D (Cyt D) is an F-actin depolymerizing drug that caps the barbed or faster-growing ends of actin filaments

(Cooper, 1987). The use of EIPA inhibited the uptake of QD/sR9 by 54% (Figure 4.9). To confirm the effective concentration of Cyt D, we used Alexa 568 - phalloidin to stain actin of Cyt D treated and control cells. At 1μg/ml, actin was successfully depolymerized in A549 cells (data not shown). Cyt D reduced the uptake of QD by 11% (Figure 4.9). Significant amount of condensed green fluorescent agglomerates were observed around cellular surface (Figure 4.9c).

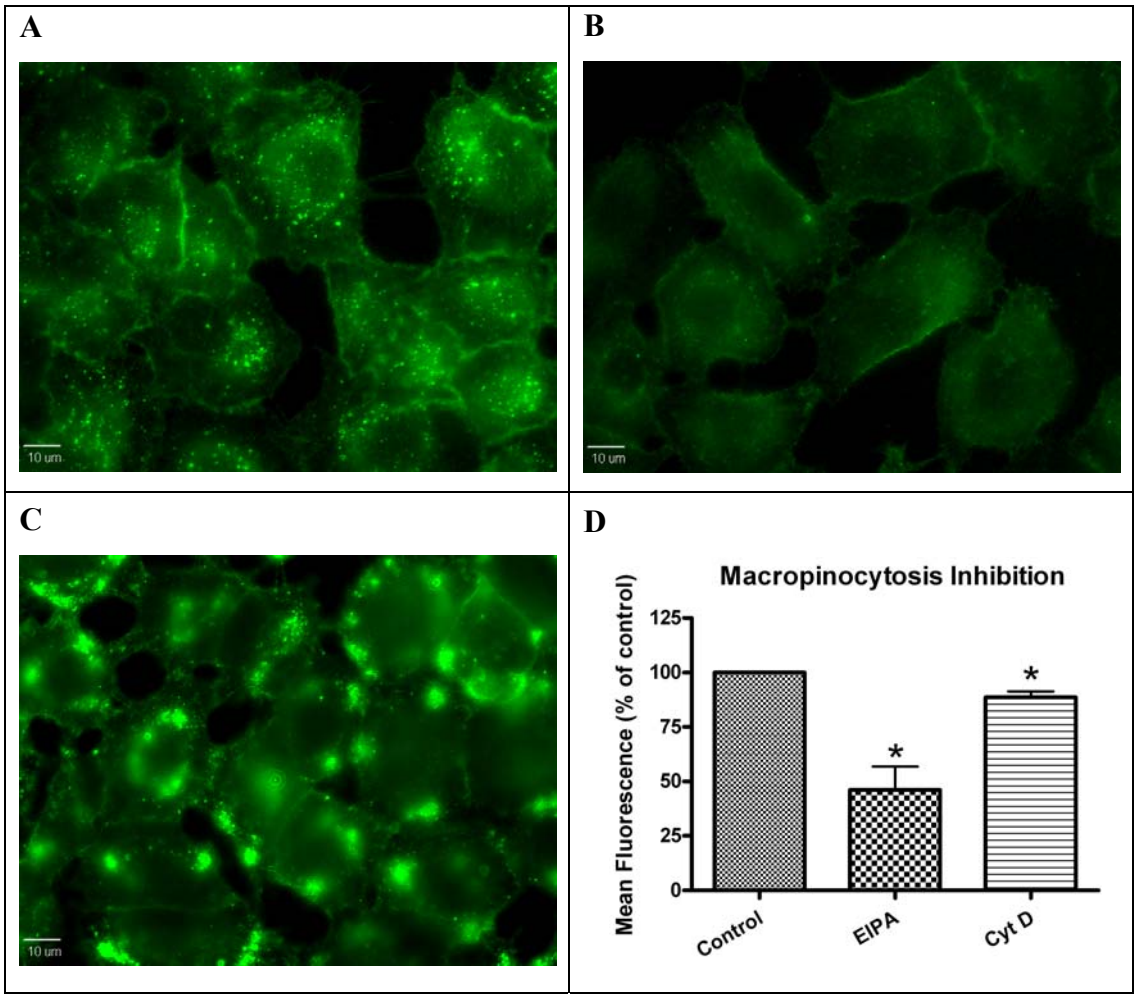

Figure 4.9. Macropinocytosis inhibition perturbed QD/sR9 internalization. A: the images of control cells. B: the images of cells pre-treated with EIPA for 30 min, then incubated with QD/sR9 for additional 1 hour. C: the images of cells pre-treated with Cyt D for 30 min, then incubated with QD/sR9 for additional 1 hour. Images represent single

plane of Z series. D: mean fluorescence intensity. Error bars represent the S.D. for 10 different fields performed in two independent experiments. Significance indicated by: *$p < 0.01$ vs. control.

4.6.5. siRNA Knockdown. Considering potential nonspecific inhibition and cytotoxicity of inhibitors, we further used the RNAi techniques to confirm the uptake mechanisms. Clathrin HC and caveolin-1 siRNA were used to knockdown clathrin-dependent and caveolin-depedent pathway, respectively. Western blot demonstrated the success of knockdown clathrin and caveolin-1 protein expression (Figure 4.10). In the clathrin HC or caveolin-1 protein knockdown cells, the uptake of QD/sR9 was not affected significantly (Figure 4.11). Clathrin siRNA data was in agreement with chlorpromazine, which indicated that the uptake was not clathrin-dependent endocytosis. Caveolin-1 siRNA data demonstrated that the caveolin-dependent pathway was not involved in QD/sR9 internalization.

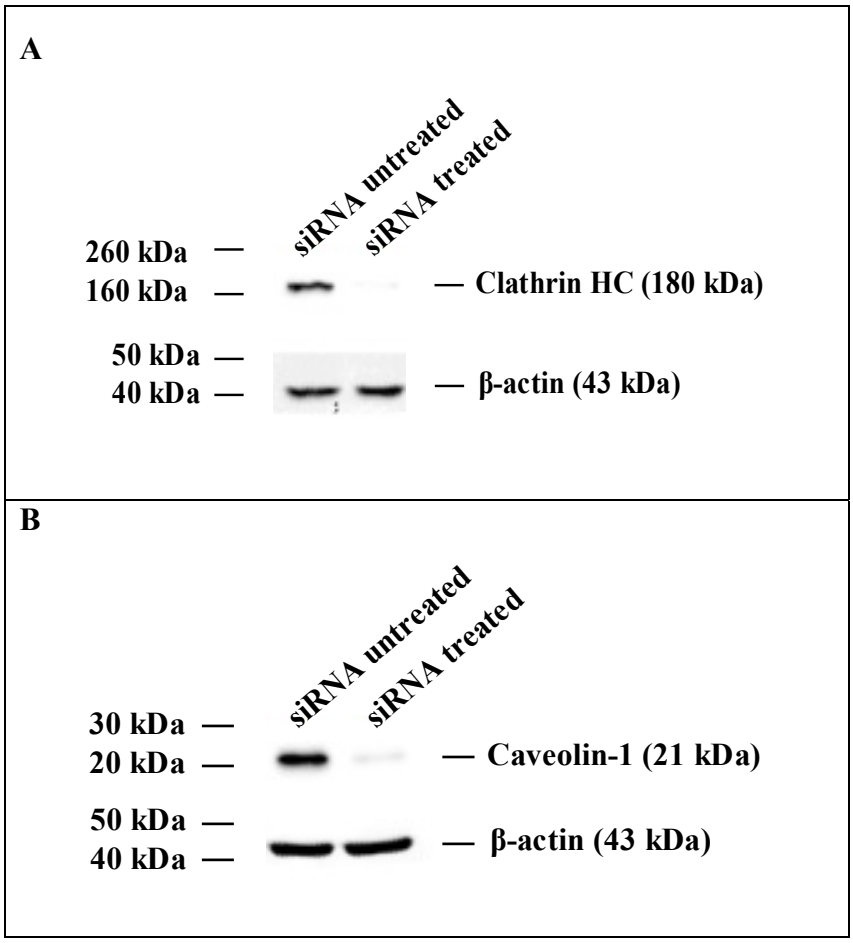

Figure 4.10. Western blot analysis. A549 cells were treated with siRNA of clathrin HC and caveolin-1 protein for 3 days, and then cells were lysed for western blot analysis. A: clathrin HC protein expression in A549 cells. B: caveolin-1 protein expression in A549 cells. β-actin was used as the control.

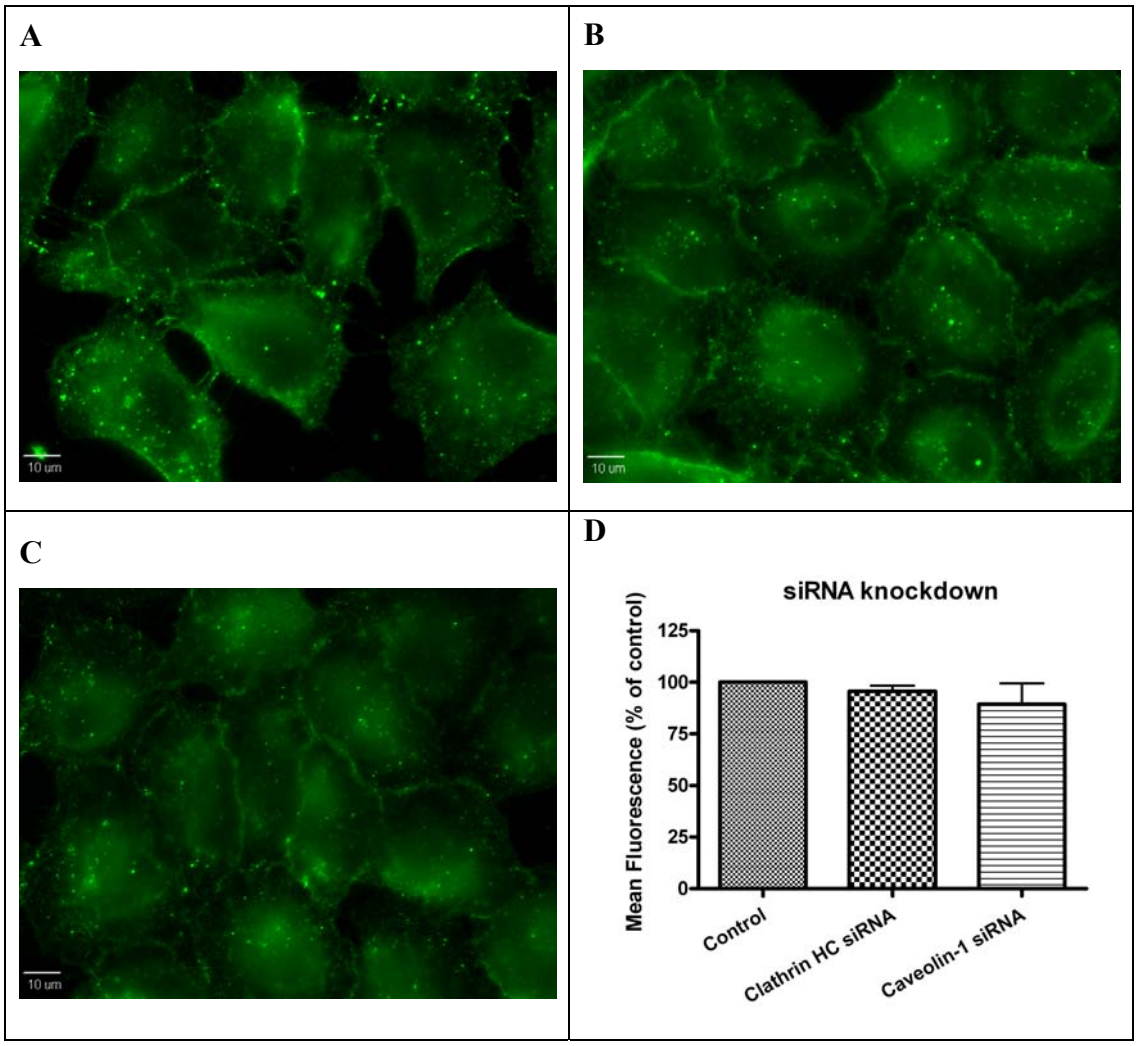

Figure 4.11. QD/sR9 uptake after knockdown of clathrin HC and caveolin-1 protein. A549 cells were treated with siRNA of clathrin HC and caveolin-1 protein for 3 days, and then cells were used for uptake studies. A: the images of control cells. B: the images of cells pre-treated with clathrin HC siRNA. C: the images of cells pre-treated with caveolin-1 siRNA. Images represent single plane of Z series. D: mean fluorescence intensity. Error bars represent the S.D. for 5 different fields performed in two independent experiments.

5. DISCUSSION

Quantum dots are emerging as a new class of fluorescent probe for cellular imaging. In comparison with organic dyes and fluorescent proteins, QDs have unique properties, such as high quantum yield and photostability which make them better suited for delivering and monitoring biomolecules. However, studies have shown that QDs are slowly internalized into the cell. Our goal was to test whether nona-arginine (sR9) can facilitate QD uptake and the mechanism of the uptake. Data from this study demonstrate that QDs are rapidly internalized into A549 cells within 5 min with the aid of sR9 (data not shown) while without the presence of sR9 QDs uptake is minimal. The enhancement of internalization is thought to be due to an electrostatic interaction between cationic nona-arginine and the negatively charged polar heads of the phospholipids of the plasma membrane (Snyder and Dowdy, 2004). Our study demonstrates that sR9 increased QD uptake up to 200nM without incurring toxicity.

QD/sR9 are internalized by endocytosis. In live cells, QD/sR9 internalization was dramatically blocked by either low temperature or a mixture of metabolic inhibitors. This indicated that the uptake of QD/sR9 was highly energy-dependent and supported that endocytosis was a major uptake process. Subsequent studies were conducted to further understand specific pathways of endocytosis.

Clathrin-dependent endocytosis is a well-characterized endocytic pathway. Treating cells with hypertonic sucrose significantly reduced QD/sR9 uptake. Although this kind of blockage is considered strong evidence of clathrin-dependent endocytosis, recent studies have shown that it also interferes with other internalization pathways, such as caveolea-dependent endocytosis and macropinocytosis (Ivanov, 2007). Thus, two specific

inhibitors, chlorpromazine and MDC, were selected for further investigation. Our data showed that MDC effectively impeded QD/sR9 internalization, while chlorpromazine at the highest possible nontoxic concentration exhibited no inhibition of QD/sR9 uptake. This contradiction might arise from two possibilities: 1) insufficient concentration of chlorpromazine; or 2) blockage of other internalization pathways by MDC. The former cannot be overcome due to apparent cytotoxicity. Blockage of other pathways by MDC treated cells might account for the possible explanation of the discrepancy. It is known that MDC is also an inhibitor of the transglutaminase family, which activates Rho GTPases, the key regulators of actin assembly and dynamics (Ivanov, 2007). Thus, MDC might block actin dependent pathways such as macropinocytosis. Because of these limitations of the inhibitor studies, we adopted siRNA to knockdown the clathrin pathway. The Western blot analysis indicated a complete knowdown of clathrin protein. The QD fluorescence intensity inside cells did not differ from the control cells indicating that clathrin-dependent pathway was not involved in QD/sR9 internalization.

Nystatin and filipin are polyene antibiotics, which create large aggregates accumulating cholesterol and thereby sequester lipid from cell membranes. Nystatin and filipin are highly selective inhibitors of the lipid raft dependent pathway because of lipid sequestering. Our data showed that both inhibitors hindered the uptake of QD/sR9, suggesting that the internalization was lipid raft dependent. Cholesterol depletion could result in blockage of several lipid raft dependent endocytic pathways, including caveolae-dependent and macropinocytosis pathways (Wadia *et al*., 2004). For further distinction, caveolin-1 siRNA was chosen to knockdown caveolin-dependent pathway. The Western blot analysis indicated a near complete knockdown of caveolin. However, live cell

imaging indicated no reduction of QD/sR9 internalization indicating a caveolin-independent pathway of QD/sR9 internalization. Collectively, QD/sR9 internalization occurred through a lipid raft dependent process, but was not mediated by clathrin and caveolin.

Macropinocytosis is a rapid, lipid raft-dependent and receptor-independent form of endocytosis. Macropinocytosis includes three essential steps: actin cytoskeleton-driven ruffle formation, closure of the ruffle into a vesicle, and dissociation of actin filaments from the vesicle (Swanson and Watts, 1995). The fluorescent intensities in cells treated with two macropinocytosis inhibitors, EIPA and Cyt D, were significantly reduced, compared to the control cells. It is worth noting that QD/sR9 was densely localized around cellular surfaces, not in cytosol. Nakase *et al*. observed a similar phenomenon that cellular R8 peptide was predominantly localized in cellular boundaries and very little punctuate staining was observed in Cyt D treated cells (Nakase *et al*., 2004). Ruan *et al.* also had the similar observation (Ruan *et al*., 2007). It is unclear how the dense aggregates affect quantitation. Further, the mechanism of the entrapment in plasma membranes remains to be investigated.

Collectively, our data show that sR9 can facilitate rapid cellular entry of QDs. The process requires energy. Chathrin and Calveolin-1 are not mediators of internalization. The major mechanism involves lipid raft and depends on macropinocytosis. Uptake mechanisms other than clathrin, caveolea, and macropinocytosis may also be involved and remain to be investigated. For instance, Rho family is the regulators of RhoA dependent and CDC42 dependent pathways (Mayor and Pagano, 2007; Sandvig *et al*., 2008).

6. FUTURE WORK

In this study, the uptake mechanism of QD/sR9 was carried out. Future work will involve several areas, including further uptake mechanism study, modifying uptake system and organelle targeting.

6.1. OTHER UPTAKE PATHWAYS

Three main pathways of endocytosis have been investigated– clathrin-dependent endocytosis, caveolea-dependent endocytosis, and macropinocytosis. Next other less-well studies pathways will be focused on. Data show that QD/sR9 uptake can be inhibited by MDC, which can block actin-dependent endocytosis via Rho family inhibition. Therefore, other pathways involved Rho family could affect QD/sR9 uptake, such as Rho A dependent pathway, CDC 42 dependent pathway.

6.2. ENDOSOMAL ESCAPING

Data show that QD/sR9 was entrapped in endosome (not shown), which will reduce the function of cargoes. Therefore, endosomal escaping is the problem that we need to resolve before we put cargoes into this delivery system. One method is using pH sensitive peptide – HA2. The α-helix of HA2 can insert into endosome membranes at low pH value, and then disrupt endosome membrane, which help QD/sR release from endosomes. The other method is modifying the surface of QDs by using PEI, which can cause proton sponge effect and let protons into endosomes resulting endosome disruption.

6.3. ORGANELLE TARGETING

After endosomal entrapment revolved, organelle targeting will be carried out. Because most drugs target nucleus or mitochondria, nucleus localizing signal or mitochondria localizing peptides will be used to target nucleus or mitochondria.

BIBLIOGRAPHY

Alivisatos AP, Gu W, Larabell C. (2005). "Quantum dots as cellular probes." Annu Rev Biomed Eng 7: 55-76.

Almofti MR, Harashima H, Shinohara Y, Almofti A, Baba Y, Kiwada H. (2003). "Cationic liposome-mediated gene delivery: biophysical study and mechanism of internalization." Arch Biochem Biophys 410(2): 246-53.

Bharali DJ, Lucey DW, Jayakumar H, Pudavar HE, Prasad PN. (2005). "Folate-receptor-mediated delivery of InP quantum dots for bioimaging using confocal and two-photon microscopy." J Am Chem Soc 127(32): 11364-71.

Bruchez M, Moronne M, Gin P, Weiss S, Alivisatos AP. (1998). "Semiconductor nanocrystals as fluorescent biological labels." Science 281(5385): 2013-6.

Chang M, Chou JC, Chen CP, Liu BR, Lee HJ. (2007). "Noncovalent protein transduction in plant cells by macropinocytosis." New Phytol 174(1): 46-56.

Conner SD and Schmid SL. (2003). "Regulated portals of entry into the cell." Nature 422(6927): 37-44.

Cooper JA. (1987). "Effects of cytochalasin and phalloidin on actin." J Cell Biol 105(4): 1473-8.

Dahan M, Laurence T, Pinaud F, Chemla DS, Alivisatos AP, Sauer M, Weiss S. (2001). "Time-gated biological imaging by use of colloidal quantum dots." Opt Lett 26(11): 825-7.

Damke H, Baba T, Warnock DE, Schmid SL. (1994). "Induction of mutant dynamin specifically blocks endocytic coated vesicle formation." J Cell Biol 127(4): 915-34.

Dietz GP and Bahr M. (2004). "Delivery of bioactive molecules into the cell: the Trojan horse approach." Mol Cell Neurosci 27(2): 85-131.

Elliott G and O'Hare P. (1997). "Intercellular trafficking and protein delivery by a herpesvirus structural protein." Cell 88(2): 223-33.

Frankel AD and Pabo CO. (1988). "Cellular uptake of the tat protein from human immunodeficiency virus." Cell 55(6): 1189-93.

Frick M, Bright NA, Riento K, Bray A, Merrified C, Nichols BJ. (2007). "Coassembly of flotillins induces formation of membrane microdomains, membrane curvature, and vesicle budding." Curr Biol 17(13): 1151-6.

Futaki S. (2002). "Arginine-rich peptides: potential for intracellular delivery of macromolecules and the mystery of the translocation mechanisms." Int J Pharm 245(1-2): 1-7.

Gong Q, Huntsman C, Ma D. (2008). "Clathrin-independent internalization and recycling." J Cell Mol Med 12(1): 126-44.

Green M and Loewenstein PM. (1988). "Autonomous functional domains of chemically synthesized human immunodeficiency virus tat trans-activator protein." Cell 55(6): 1179-88.

Hansen CG and Nichols BJ. (2009). "Molecular mechanisms of clathrin-independent endocytosis." J Cell Sci 122(Pt 11): 1713-21.

Hansen SH, Sandvig K, van Deurs B. (1993). "Clathrin and HA2 adaptors: effects of potassium depletion, hypertonic medium, and cytosol acidification." J Cell Biol 121(1): 61-72.

Heitz F, Morris MC, Divita G. (2009). "Twenty years of cell-penetrating peptides: from molecular mechanisms to therapeutics." Br J Pharmacol 157(2): 195-206.

Hewlett LJ, Prescott AR, Watts C. (1994). "The coated pit and macropinocytic pathways serve distinct endosome populations." J Cell Biol 124(5): 689-703.

Hoshino AK, Fujioka K, Oku T, Nakamura S, Suga M, Yamaguchi Y, Suzuki K, Yasuhara M, Yamamoto K. (2004). "Quantum dots targeted to the assigned organelle in living cells." Microbiol Immunol 48(12): 985-94.

Ivanov AI. (2007). Exocytosis and Endocytosis Humana press.

Joliot A, Pernelle C, Deagostini-Bazin H, Prochiantz A. (1991). "Antennapedia homeobox peptide regulates neural morphogenesis." Proc Natl Acad Sci U S A 88(5): 1864-8.

Kaplan IM, Wadia JS, Dowdy SF. (2005). "Cationic TAT peptide transduction domain enters cells by macropinocytosis." J Control Release 102(1): 247-53.

Khalil IA, Kogure K, Futaki S, Harashima H. (2006). "High density of octaarginine stimulates macropinocytosis leading to efficient intracellular trafficking for gene expression." J Biol Chem 281(6): 3544-51.

Kim S, Lim YT, Soltesz EG, De Grand AM, Lee J, Nakayama A, Parker JA, Mihaljevic T, Laurence RG, Dor DM, Cohn LH, Bawendi MG, Frangioni JV. (2004). "Near-infrared fluorescent type II quantum dots for sentinel lymph node mapping." Nat Biotechnol 22(1): 93-7.

Lai CY, Trewyn BG, Jeftinija DM, Jeftinija K, Xu S, Jeftinija S, Lin VS. (2003). "A mesoporous silica nanosphere-based carrier system with chemically removable CdS nanoparticle caps for stimuli-responsive controlled release of neurotransmitters and drug molecules." J Am Chem Soc 125(15): 4451-9.

Lindsay MA. (2002). "Peptide-mediated cell delivery: application in protein target validation." Curr Opin Pharmacol 2(5): 587-94.

Mayor S and Pagano RE. (2007). "Pathways of clathrin-independent endocytosis." Nat Rev Mol Cell Biol 8(8): 603-12.

Maysinger D, Lovric J, Eisenberg A, Savic R. (2007). "Fate of micelles and quantum dots in cells." Eur J Pharm Biopharm 65(3): 270-81.

Michalet X, Pinaud FF, Bentolila LA, Tsay JM, Doose S, Li JJ, Sundaresan G, Wu AM, Gambhir SS, Weiss S. (2005). "Quantum dots for live cells, in vivo imaging, and diagnostics." Science 307(5709): 538-44.

Minet O, Dressler C, Beuthan J. (2004). "Heat stress induced redistribution of fluorescent quantum dots in breast tumor cells." J Fluoresc 14(3): 241-7.

Mousavi SA, Malerod L, Berg T, Kjeken R. (2004). "Clathrin-dependent endocytosis." Biochem J 377(Pt 1): 1-16.

Nakase I, Niwa M, Takeuchi T, Sonomura K, Kawabata N, Koike Y, Takehashi M, Tanaka S, Ueda K, Simpson JC, Jones AT, Sugiura Y, Futaki S. (2004). "Cellular uptake of arginine-rich peptides: roles for macropinocytosis and actin rearrangement." Mol Ther 10(6): 1011-22.

Ozkan M. (2004). "Quantum dots and other nanoparticles: what can they offer to drug discovery?" Drug Discov Today 9(24): 1065-71.

Panicker AK, Buhusi M, Erickson A, Maness PF. (2006). "Endocytosis of beta1 integrins is an early event in migration promoted by the cell adhesion molecule L1." Exp Cell Res 312(3): 299-307.

Parton RG and Simons K. (2007). "The multiple faces of caveolae." Nat Rev Mol Cell Biol 8(3): 185-94.

Parungo CP and Colson YL. (2005a). "Sentinel lymph node mapping of the pleural space." Chest 127(5): 1799-804.

Parungo CP, Ohnishi S, Kim SW, Kim S, Laurence RG, Soltesz EG, Chen FY, Colson YL, Cohn LH, Bawendi MG, Frangioni JV. (2005b). "Intraoperative identification of esophageal sentinel lymph nodes with near-infrared fluorescence imaging." J Thorac Cardiovasc Surg 129(4): 844-50.

Phonphok Y and Rosenthal KS. (1991). "Stabilization of clathrin coated vesicles by amantadine, tromantadine and other hydrophobic amines." FEBS Lett 281(1-2): 188-90.

Pujals S, Fernandez-Carneado J, Lopez-Iglesias C, Kogan MJ, Giralt E. (2006). "Mechanistic aspects of CPP-mediated intracellular drug delivery: relevance of CPP self-assembly." Biochim Biophys Acta 1758(3): 264-79.

Ruan G, Agrawal A, Marcus AI, Nie S. (2007). "Imaging and tracking of tat peptide-conjugated quantum dots in living cells: new insights into nanoparticle uptake, intracellular transport, and vesicle shedding." J Am Chem Soc 129(47): 14759-66.

Sandvig K, Torgersen ML, Raa HA, van Deurs B. (2008). "Clathrin-independent endocytosis: from nonexisting to an extreme degree of complexity." Histochem Cell Biol 129(3): 267-76.

Schnitzer JE, Oh P, Pinney E, Allard J. (1994). "Filipin-sensitive caveolae-mediated transport in endothelium: reduced transcytosis, scavenger endocytosis, and capillary permeability of select macromolecules." J Cell Biol 127(5): 1217-32.

Schwarze SR, Hruska KA, Dowdy SF. (2000). "Protein transduction: unrestricted delivery into all cells?" Trends Cell Biol 10(7): 290-5.

Snyder EL and Dowdy SF. (2004). "Cell penetrating peptides in drug delivery." Pharm Res 21(3): 389-93.

Soltesz EG and Kim S. (2006). "Sentinel lymph node mapping of the gastrointestinal tract by using invisible light." Ann Surg Oncol 13(3): 386-96.

Soltesz EG and Kim S. (2005). "Intraoperative sentinel lymph node mapping of the lung using near-infrared fluorescent quantum dots." Ann Thorac Surg 79(1): 269-77; discussion 269-77.

Sverdlov M, Shajahan AN, Minshall RD. (2007). "Tyrosine phosphorylation-dependence of caveolae-mediated endocytosis." J Cell Mol Med 11(6): 1239-50.

Swanson JA and Watts C. (1995). "Macropinocytosis." Trends Cell Biol 5(11): 424-8.

Tunnemann G, Ter-Avetisyan G, Martin RM, Stockl M, Herrmann A, Cardoso MC. (2008). "Live-cell analysis of cell penetration ability and toxicity of oligo-arginines." J Pept Sci 14(4): 469-76.

Vives E, Brodin P, Lebleu B. (1997). "A truncated HIV-1 Tat protein basic domain rapidly translocates through the plasma membrane and accumulates in the cell nucleus." J Biol Chem 272(25): 16010-7.

Wadia JS and Dowdy SF. (2002). "Protein transduction technology." Curr Opin Biotechnol 13(1): 52-6.

Wadia JS, Stan RV, Dowdy SF. (2004). "Transducible TAT-HA fusogenic peptide enhances escape of TAT-fusion proteins after lipid raft macropinocytosis." Nat Med 10(3): 310-5.

Wang LH, Rothberg KG, Anderson RG. (1993). "Mis-assembly of clathrin lattices on endosomes reveals a regulatory switch for coated pit formation." J Cell Biol 123(5): 1107-17.

Wang YH, Chen CP, Chan MH, Chang M, Hou YW, Chen HH, Hsu HR, Liu K, Lee HJ. (2006). "Arginine-rich intracellular delivery peptides noncovalently transport protein into living cells." Biochem Biophys Res Commun 346(3): 758-67.

Wang YH, Hou YW, Lee HJ. (2007). "An intracellular delivery method for siRNA by an arginine-rich peptide." J Biochem Biophys Methods 70(4): 579-86.

Wu X, Liu H, Liu J, Haley KN, Treadway JA, Larson JP, Ge N, Peale F, Bruchez MP. (2003). "Immunofluorescent labeling of cancer marker Her2 and other cellular targets with semiconductor quantum dots." Nat Biotechnol 21(1): 41-6.

Xue FL, Chen JY, Guo J, Wang CC, Yang WL, Wang PN, Lu DR. (2007). "Enhancement of intracellular delivery of CdTe quantum dots (QDs) to living cells by Tat conjugation." J Fluoresc 17(2): 149-54.

Yao D, Ehrlich M, Henis YI, Leof EB. (2002). "Transforming growth factor-beta receptors interact with AP2 by direct binding to beta2 subunit." Mol Biol Cell 13(11): 4001-12.

Zhang, L. W. and N. A. Monteiro-Riviere (2009). "Mechanisms of quantum dot nanoparticle cellular uptake." Toxicol Sci 110(1): 138-55.

Ziegler A, Nervi P, Durrenberger M, Seelig J. (2005). "The cationic cell-penetrating peptide CPP(TAT) derived from the HIV-1 protein TAT is rapidly transported into living fibroblasts: optical, biophysical, and metabolic evidence." Biochemistry 44(1): 138-48.

VITA

Yi Xu was born on December 19th, 1974, in Handan, Hebei Province, P.R China. She received her Bachelor of Medicine Degree in Clinical Medicine, School of Medicine (formerly Nanjing Railway Medical College), Southeast University, Nanjing, Jiangsu, P.R.China in 1998. She worked as a resident in Fengtai Hospital, Beijing, from 1998 to 2001. In 2001, she entered the Capital University of Medical Sciences, Beijing, P.R.China and received her Master of Medicine Degree in Obstetrics and Gynecology in 2004. She worked in the Reproduction and Genetics Center of Beijing Obstetrics and Gynecology Hospital from 2004 to 2005. In June 2005, she came to United States with her husband. In May 2007, she enrolled in the Department of Biological Sciences pursing her Master Degree at the Missouri University of Science & Technology (formerly University of Missouri-Rolla), and received her Master Degree in December 2009.